J. Phys. D: Appl. Phys. **41** (2008) 015104 (7pp) doi:10.1088/0022-3727/41/1/015104

Characterization of luminescent samarium doped HfO_2 coatings synthesized by spray pyrolysis technique

C Chacón-Roa[1], J Guzmán-Mendoza[1,2], M Aguilar-Frutis[1], M García-Hipólito[2], O Alvarez-Fragoso[2] and C Falcony[3]

[1] Centro de Investigación en Ciencia Aplicada y Tecnología Avanzada-IPN, Legaria 694, Col. Irrigación, C.P. 11500, México D.F., Mexico
[2] Departamento de Materiales Metálicos y Cerámicos, Instituto de Investigaciones en Materiales, Universidad Nacional Autónoma de México, A.P. 70-360 Coyoacán 04510, México, D.F., Mexico
[3] Departamento de Física, CINVESTAV-IPN, A. P. 14-740, 07000 México D.F., Mexico

E-mail: maguilarf@ipn.mx

Received 14 June 2007, in final form 2 October 2007
Published 12 December 2007
Online at stacks.iop.org/JPhysD/41/015104

Abstract
Trivalent samarium (Sm^{3+}) doped hafnium oxide (HfO_2) films were deposited using the spray pyrolysis deposition technique. The films were deposited on Corning glass substrates at temperatures ranging from 300 to 550 °C using chlorides as raw materials. Films, mostly amorphous, were obtained when deposition temperatures were below 350 °C. However, for temperatures higher than 400 °C, the films became polycrystalline, presenting the HfO_2 monoclinic phase. Scanning electron microscopy of the films revealed a rough surface morphology with spherical particles. Also, electron energy dispersive analysis was performed on these films. The photoluminescence and cathodoluminescence characteristics of the $HfO_2 : SmCl_3$ films, measured at room temperature, exhibited four main bands centred at 570, 610, 652 and 716 nm, which are due to the well-known intra-4f transitions of the Sm^{3+} ion. It was found that the overall emission intensity rose as the deposition temperature was increased. Furthermore, a concentration quenching of the luminescence intensity was also observed.

1. Introduction

Transition metal oxides, such as hafnium oxide (HfO_2), have attracted significant attention because of their potential applications. HfO_2 can be used as a gas sensor [1] and waveguide [2], as well as a protective coating, due to its thermal stability and hardness [3, 4]. Up to now, one of the most important applications of HfO_2 is probably in the microelectronic industry. HfO_2 is studied as a high-k gate dielectric layer with a relatively high index of refraction and a wide energy band gap. These properties make HfO_2 a good candidate for applications in metal-oxide-semiconductor devices for the next generation [5, 6]. The wide band gap of HfO_2 makes it transparent over a wide spectroscopic range: from the ultraviolet to the mid-infrared [7]. Furthermore, HfO_2 has been employed in optical coating applications such as high-reflectivity mirrors, anti-reflection coatings, filters and beamsplitters [8, 9]. In addition, the large energy band gap and the low phonon frequencies make HfO_2 an appropriate host matrix for being doped with rare earth activators [10, 11]. Efficient luminescent materials have wide applications in electroluminescent flat panel displays; colour plasma display panels, scintillators, cathode ray tubes, fluorescent lamps, lasers, etc. In recent years the study of luminescent materials based on HfO_2 has been intensified. Some groups have studied the optical properties of doped and undoped HfO_2 [12–14]. Specifically, some studies on rare earth and Mn doped HfO_2 films have been recently reported [12, 15–17]. One of the most important properties of rare earth ions doped compounds is the very narrow absorption and emission band arising from the parity-forbidden intraconfigurational 4f–4f transitions. As a result, trivalent rare earth ions possess very good luminescent characteristics (high colour purity). In particular, luminescence of samarium ions in solids has attracted much attention in recent years to produce reddish-orange emitting phosphors for colour display panels [18, 19],

for thermoluminescent materials [20] and for materials with long-lasting properties [21], etc. Hafnium oxide films have been deposited by a variety of techniques; these include atomic layer epitaxy [22], chemical vapour deposition [23], conventional electron beam evaporation [24], ion-assisted electron beam evaporation [7], sputtering [25] and ultrasonic spray pyrolysis (USP) [26]. USP is a processing technique used in research to prepare thin and thick films and powders. Unlike many other film deposition techniques, USP represents a very simple and relatively cost-effective processing method (with regard to equipment costs). It is a simple process for depositing films of any composition, in particular oxides and sulfides. USP does not require high-quality substrates or chemicals. The method has been employed for the deposition of dense or porous films and for several types of powder production. Furthermore, multilayered films can be easily prepared using this versatile technique. The precursor solutions used in this technique are obtained from inorganic and organic salts such as chlorides, nitrates, acetates, acetylacetonates, ethoxides and butoxides dissolved in deionized water, alcohol or other organic solvents [27]. USP has been applied to deposit a large variety of films, those with luminescent properties standing out such as Al_2O_3, ZrO_2, $ZnAl_2O_4$ and HfO_2 doped with rare earth or transition elements (Mn) [17, 28, 29, 30].

In this work the luminescence (PL and CL) features of $HfO_2 : SmCl_3$ coatings synthesized by the USP technique are studied. Also, the characteristics of the surface morphology, the crystalline structure and the chemical composition of the luminescent films, as a function of the deposition temperature and doping concentration, are described.

2. Experimental details

The USP technique was used to deposit samarium doped HfO_2 films. The USP deposition system consists of a precursor solution, an ultrasonic atomizer, a substrate heater and a temperature controller. The details of this technique have been described previously [31]. The starting reagents to deposit $HfO_2 : Sm^{3+}$ films were $SmCl_3 \cdot 6H_2O$ and $HfCl_2O \cdot 8H_2O$; a 0.7 molar concentration solution was prepared in deionized water as a solvent. The impurity concentrations in the spray solution were 1, 3, 5, 10 and 20 a/o (atomic per cent, in relation to the hafnium content). Deposition temperatures (T_s) were in the range from 300 to 550 °C. Corning glass pieces ($1 \times 1.5\,cm^2$) were used as substrates. The carrier gas was filtered air and the flow rate was $8\,l\,min^{-1}$. The deposition time was 5–6 min for all the samples in order to get films with almost the same thickness. The thickness of the films was approximately $10 \pm 5\,\mu m$ (deposition rate $\sim 2\,\mu m\,min^{-1}$), as measured by a Sloan Dektak IIA profilometer (with an accuracy of $\pm 0.03\,\mu m$). The film thickness variation of up to 50% was because of the large roughness presented by these films. The microstructure of the films was observed in a Cambridge-Leica scanning electron microscope (SEM), model Stereoscan 440. The SEM is equipped with an energy dispersive spectroscopy system (EDS), from Oxford, model Pentafet, that uses a Si-Li detector. The crystalline structure of the coatings was evaluated in a Siemens D-5000 diffractometer (Cu Kα,λ= 1.5406 Å). Cathodoluminescence (CL) measurements were performed in a stainless steel vacuum chamber with a cold cathode electron gun (Luminoscope, model ELM-2 MCA, Relion Co.). Samples were placed inside the vacuum chamber and evacuated to $\leqslant 10^{-3}$ Torr. The electron beam was deflected through a 90° angle to bombard the luminescent films normal to the surface. The emitted light from the sample was coupled to an optical fibre bundle leading to a Perkin-Elmer LS50B fluorescence spectrophotometer. The photoluminescence excitation (PLE) and emission (PL) spectra were obtained using the spectrophotometer cited above. Both PL and CL spectra were obtained at room temperature and radiation of 270 nm (from excitation spectrum) was found to be suitable as an excitation source for the PL measurements.

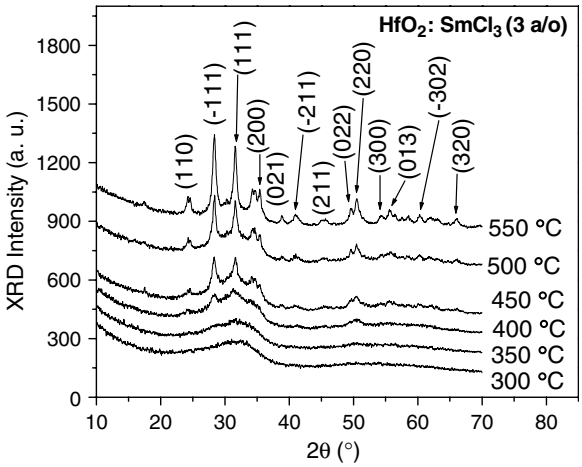

Figure 1. X-ray diffractograms for $HfO_2 : Sm^{3+}$ (3 a/o) films grown at different T_s: 300, 350, 400, 450, 500 and 550 °C.

3. Results and discussion

In figure 1, the results of XRD measurements, carried out on $HfO_2 : SmCl_3$ (3 a/o) films, are shown. Diffraction patterns for samples deposited at T_s from 300 to 550 °C are exhibited. For low deposition temperatures (300, 350 °C), the hafnium oxide coatings have poor crystallinity. It seems that for these deposition temperatures the films are amorphous and/or nanocrystalline. For higher substrate temperatures, the films show peaks which correspond to the monoclinic phase of hafnium oxide (referenced as JCPDS 431017). Sharper diffraction peaks at high T_s could indicate an increase in the crystallite's size. The relative atomic percentages of oxygen, chlorine, hafnium, and samarium are shown in table 1 as a function of the deposition temperature for films deposited with 3 a/o of Sm and in table 2 as a function of the Sm doping concentration in films that were deposited at 550 °C. Even though EDS is not a quantitative technique it is useful to estimate the chemical composition of the films. It is possible to observe from table 1 that the oxygen content in the films increases slightly when the substrate temperature is raised from 300 to 550 °C, and at the same time, the percentage of chlorine is decreased. It seems that chlorine is released as a volatile gas, and more oxygen is incorporated. The hafnium and samarium

Table 1. Atomic per cent content of oxygen, chlorine, hafnium and samarium in the Sm-doped hafnium oxide films as determined by EDS for different substrate temperatures. In this case, the $SmCl_3$ concentration in the spraying solution was 3 a/o.

T_s (°C)	O	Cl	Hf	Sm
300	67.0	10.3	21.9	0.8
350	68.7	7.9	22.7	0.7
400	68.1	4.5	26.5	0.9
450	68.7	4.8	25.9	0.6
500	71.6	3.2	24.5	0.7
550	72.9	2.6	23.8	0.7

Table 2. Atomic per cent content of oxygen, chlorine, hafnium and samarium in the Sm-doped hafnium oxide films as measured by EDS for different $SmCl_3$ concentrations in the spraying solution. The substrate temperature was 550 °C.

C_{Sm} (a/o)	O	Cl	Hf	Sm
0	69.2	3.3	27.5	0
1	69.7	3.2	26.8	0.3
3	72.9	2.6	23.8	0.7
5	71.9	2.9	23.9	1.3
10	71.0	4.4	22.7	1.9
20	73.5	3.2	19.7	3.6

contents remain almost constant in this temperature range. Furthermore, it is observed in table 2 that when the substrate temperature is kept at 550 °C and the amount of Sm in the solution is varied, the amount of chlorine in the films remains constant. The hafnium relative content, on the other hand, decreases while the Sm increases suggesting that trivalent samarium ions substitute tetravalent hafnium; therefore the chlorine ions in the film could act as charge compensators to preserve the electrical neutrality.

In figure 2, SEM micrographs of the surface morphology of $HfO_2 : SmCl_3$ (3 a/o) coatings are presented. It is possible to observe rough, but continuous films with good adherence to the substrate. The SEM micrographs correspond to the samples deposited at 300 °C (*a*), 350 °C (*b*), 400 °C (*c*), 500 °C (*d*), 550 °C (*e*), 600 °C (*f*). In addition, a cross section view of a film deposited at 500 °C (*g*) is also shown in figure 2. It is observed that the surface morphology of the films depends on the deposition temperature. Layers deposited at 300 °C present rough surfaces formed by a material not completely processed and it also is possible to observe some holes and cracks; presumably in this case the substrate thermal energy is not enough to process the material completely to form closed and compacted surfaces. Films deposited at 350 °C present an open network formed by 'veins' and is porous, but apparently with more compacted zones. As the deposition temperature increases (from 400 to 550 °C), the network is closed, crack-free and apparently more compacted, although rough surfaces are still observed. Probably these characteristics are obtained because at a higher substrate temperature the deposited precursors have a larger surface kinetic energy, which produces a more complete pyrolytic reaction of the reactant materials which results in a more compacted film. In addition, in samples deposited at 500 and 550 °C, it is possible to distinguish a rough and continuous surface finely granulated with some spherical particles upon the surface. Figure 2(*f*) shows the surface morphology of a film deposited at a substrate temperature of 600 °C; this resulted in a powdery material, porous (with some spherical exploded particles) and non-adherent to the substrate. These characteristics are probably due to sudden evaporation of the solvent because at those relatively high temperatures the chemical reaction is carried out in the vapour phase in a nearby region to the substrate, producing in this way only a fine powder (which falls on the substrate) and not a solid coating. In figure 2(*g*), a cross section of the sample deposited at 500 °C is exhibited. Here it is possible to observe a nodular growth of the film more than a columnar one. It is possible to observe that the coating is formed by two sections: one constituted by a 'solid' layer of approximately 0.2 μm and above the previous one, another section composed of spherical particles of diverse sizes (typically $\sim$1 μm). This phenomenon has been interpreted [32] as an initial stage in which the pyrolytic reaction is such that the gaseous by-products are released efficiently out of the deposited material when this process occurs directly on the glass substrate. As the deposited film becomes thick, the removal of the gaseous by-products is less efficient giving place to bubble-like formations (spheres) on the surface of the film. As the deposition temperature increases (from 500 to 550 °C), it is possible to observe some broken spheres due to the internal stress of the trapped gases. The value of the thickness and characteristics observed by SEM is similar to the one measured by profilometry.

The PLE spectrum of the $HfO_2 : SmCl_3$ coatings synthesized at 550 °C and with 3 a/o of $SmCl_3$ in the spraying solution is shown in figure 3. The emission wavelength was fixed at 610 nm. It is possible to distinguish a main asymmetrical broad band with the wavelength ranging from 225 to 300 nm. In this broad band a main peak is noticed, centred at 270 nm, and a shoulder centred at 252 nm. This broad band whose maximum value is located at 270 nm can be attributed to the charge transfer transition between $O^{2-} \rightarrow Sm^{3+}$ [21]. Then, the 270 nm wavelength radiation was chosen to excite the photoluminescence of the coatings studied in this work.

In figure 4 a representative PL emission spectrum for Sm-doped hafnium oxide films is shown. This spectrum exhibits four main bands centred at 570 nm ($^4G_{5/2} \rightarrow {}^6H_{5/2}$), 610 nm ($^4G_{5/2} \rightarrow {}^6H_{7/2}$), 652 nm ($^4G_{5/2} \rightarrow {}^6H_{9/2}$) and 716 nm ($^4G_{5/2} \rightarrow {}^6H_{11/2}$), which are all connected to the well-known intra-4f transitions of Sm^{3+} ions from the excited to the lower levels [33]. As can be observed, the emission at 610 nm is the strongest one. From this, it can be said that the excited material shows a reddish colour. In this case the films were prepared at a substrate temperature of 550 °C and a doping concentration of 3 a/o in the spraying solution. It is commonly accepted that the magnetic dipole (md) allowed transitions obey the selection rule $\Delta J = 0, \pm 1$. Then the transition $^4G_{5/2} \rightarrow {}^6H_{5/2}$ according to the first condition rule ($\Delta J = 0$) is a natural (md) allowed transition, whose intensity remains without change relative to the host matrix. The $^4G_{5/2} \rightarrow {}^6H_{7/2}$ transition, ($\Delta J = \pm 1$), has also been labelled as a (md) allowed transition, but it is electric dipole (ed) dominated. Then, it can be stated that the latter transition has both (md) and

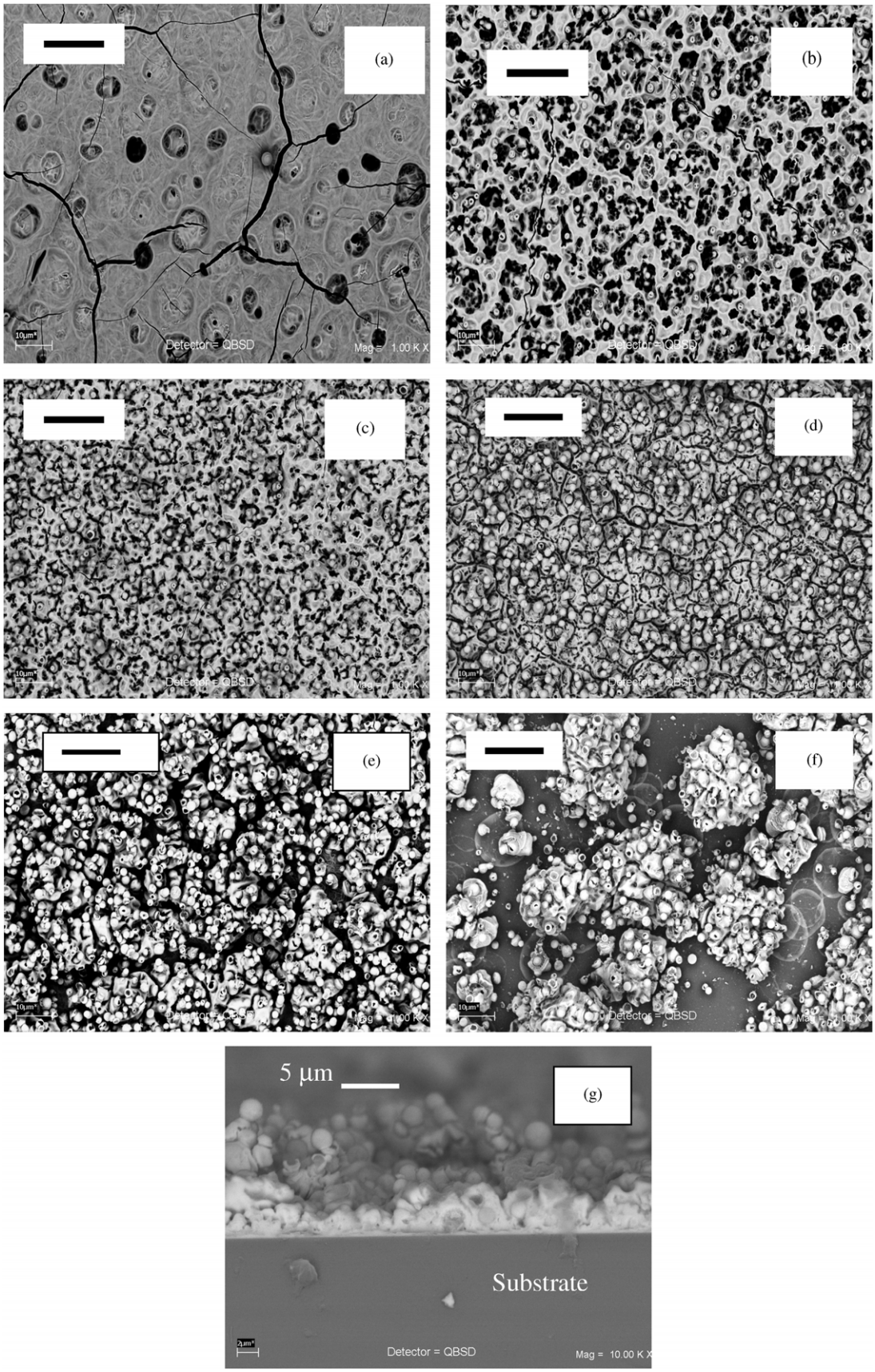

Figure 2. SEM micrographs of the surface morphology of $HfO_2 : Sm^{3+}$ coatings as a function of T_s: (*a*) 300 °C, (*b*) 350 °C, (*c*) 400 °C, (*d*) 500 °C, (*e*) 550 °C, (*f*) 600 °C and (*g*) cross section image of the sample deposited at 500 °C. Except in (*g*), the length of the black bar represents 12 μm.

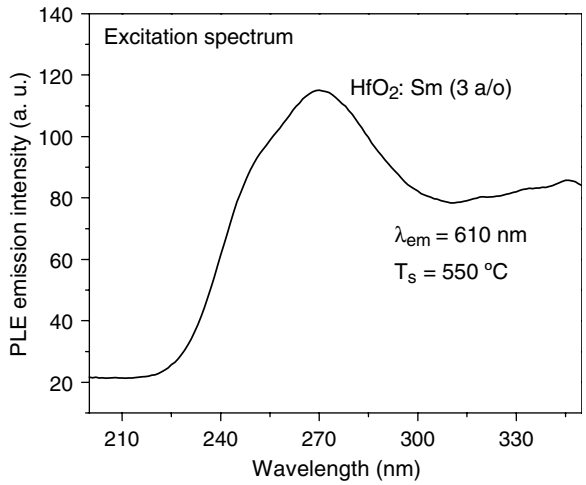

Figure 3. Excitation spectrum for $HfO_2 : Sm^{3+}$ (3 a/o) films deposited at 550 °C. The emission wavelength was fixed at 610 nm.

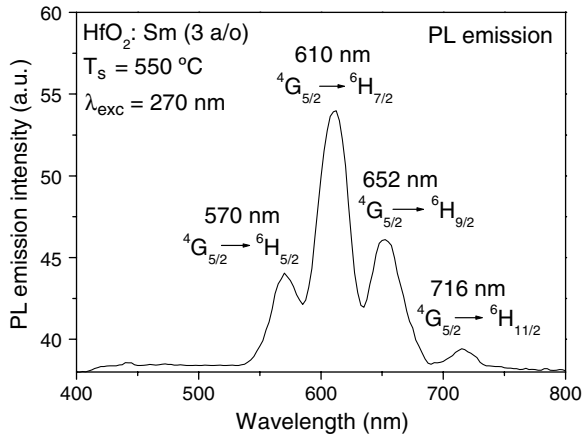

Figure 4. Representative PL emission spectrum of $HfO_2 : Sm^{3+}$ (3 a/o) films grown at 550 °C. The excitation wavelength was 270 nm.

(ed) components. The $^4G_{5/2} \rightarrow {}^6H_{9/2}$ transition is purely (ed), the one which is sensitive to the crystal field [34, 35]. Usually, the intensity ratio of (ed) to (md) allowed transitions is used to measure the symmetry of the local environment of trivalent 4f ions. The greater the intensity of the (ed) transition, the more the asymmetry nature [36]. In this study, the $^4G_{5/2} \rightarrow {}^6H_{9/2}$ (ed) transition, concerning the electronic levels of Sm^{3+} ions, is more intense than the $^4G_{5/2} \rightarrow {}^6H_{5/2}$ (md) one, indicating the asymmetric nature of the host matrix.

Figure 5 shows the 610 nm ($^4G_{5/2} \rightarrow {}^6H_{7/2}$ electronic transition) emission intensity behaviour as a function of the deposition temperature. The PL emissions rise when the deposition temperature increases. The maximum emission intensity was reached for the sample deposited at 550 °C, probably due to an improved crystallization of the host material and/or to the reduction of chlorine left in the coating. Both effects will produce a better incorporation and distribution of samarium ions as an atomic impurity into the host matrix, which would result in an increase in the PL emission as the deposition temperature is increased. In this case, the value of impurity concentration in the spraying solution was of 3 a/o and the excitation wavelength was at 270 nm.

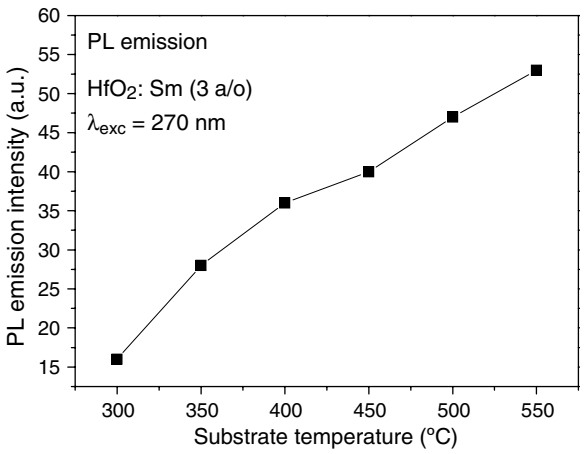

Figure 5. PL emission intensity behaviour of the peak centred at 610 nm, as a function of the substrate temperature for $HfO_2 : Sm^{3+}$ (3 a/o) coatings. The excitation wavelength was fixed at 270 nm.

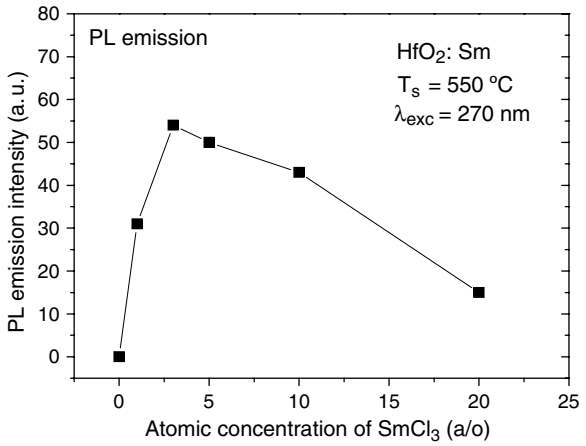

Figure 6. PL emission intensity tendency of the peak centred at 610 nm, as a function of the doping concentration for $HfO_2 : Sm^{3+}$ coatings. The substrate temperature was 550 °C and the excitation wavelength was fixed at 270 nm.

The dependence of PL intensity in the 610 nm peak for Sm-doped hafnium oxide films, as a function of doping concentration, is shown in figure 6. The emission intensity shows a maximum at 3 a/o of $SmCl_3$ in the spraying solution. Concentration quenching is observed for this case [37]. Again, the wavelength of the excitation was at 270 nm and the substrate temperature was 550 °C.

An orange-reddish PL emission could easily be appreciated with the naked eye in normal room light from $HfO_2 : Sm^{3+}$ samples when excited with a 4 W UV-mercury lamp (254 nm); this gives an idea, if not quantitatively at least qualitatively, of the strength of the PL emission.

The CL emission spectra of $HfO_2 : Sm^{3+}$ coatings, deposited under different substrate temperatures, are shown in figure 7 as a function of the wavelength. These spectra exhibit main bands centred at 567 nm, 602 nm and 647 nm and a small peak localized at 712 nm, which correspond, within the expected wavelength spreading, to transitions from the $^4G_{5/2}$ level to the $^6H_{5/2}$, $^6H_{7/2}$, $^6H_{9/2}$ and $^6H_{11/2}$ levels of the ground state of the Sm^{+3} ions, respectively, as in the case

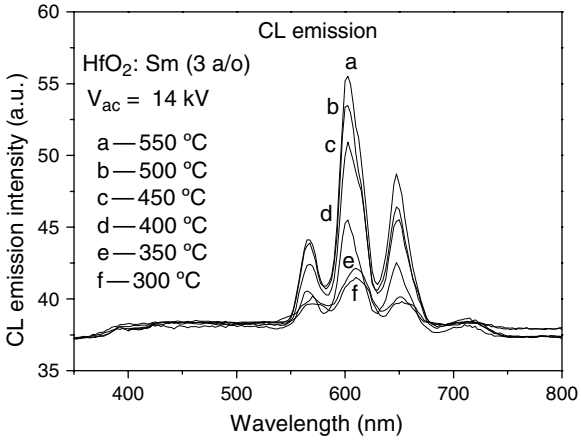

Figure 7. CL emission spectra of $HfO_2 : Sm^{3+}$ (3 a/o) coatings as a function of the wavelength for samples deposited at different substrate temperatures. The electron accelerating voltage was 14 kV.

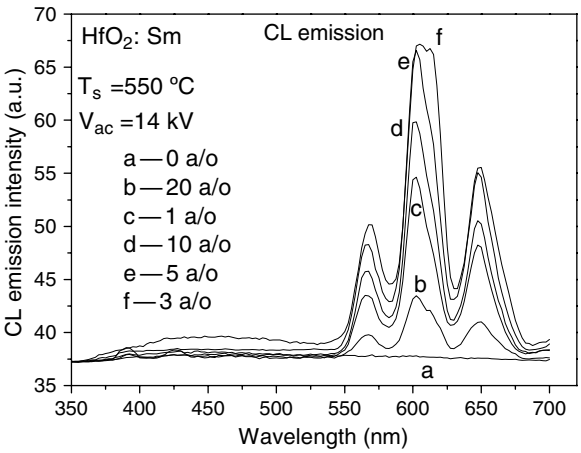

Figure 8. Tendency of the CL emission intensity, as a function of the wavelength for $HfO_2 : Sm^{3+}$ films with variations in the concentration doping. Here, the coatings were deposited at 550 °C and the applied electron accelerating potential was 14 kV.

of PL measurements. Once again, the strongest emission corresponds to red $^4G_{5/2} \rightarrow {}^6H_{7/2}$ electronic transition. The CL emission intensities rise when the substrate temperatures are increased. These CL results confirm the conclusion drawn from the PL measurements suggesting a reduction on the structural defects and in the crystallite growth in the films, favouring radiative recombination mechanisms. For this case, the electron accelerating voltage was 14 kV and the doping concentration in the spraying solution was fixed at 3 a/o of $SmCl_3$.

Figure 8 shows the behaviour of the CL emission intensity as a function of the wavelength, for films with different doping concentrations. Here, the coatings were deposited at 550 °C and the applied electron accelerating potential was of 14 kV. As the Sm concentration is increased, a quenching effect of the overall CL emission is observed. The maximum emission intensity is obtained for 3 a/o of samarium chloride in the spraying solution, as in the case of PL. This concentration quenching effect has been explained in terms of an increment in the migration of the excitation energy by resonant energy transfer between rare earth activators. Furthermore, it is

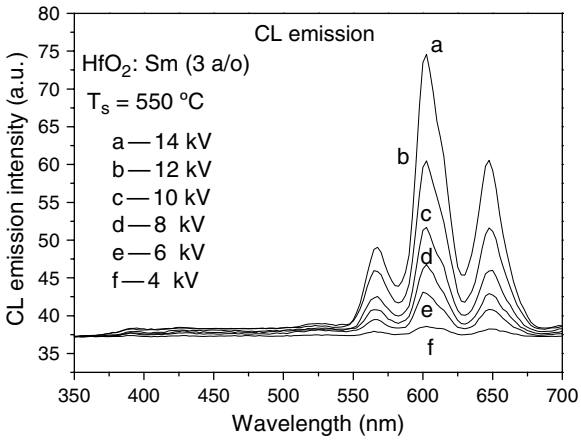

Figure 9. The behaviour of the CL emission intensity spectra for $HfO_2 : Sm^{3+}$ (3 a/o) films, as a function of the wavelength, with accelerating beam voltages in the range from 4 to 14 kV. In this case the films were deposited at 550 °C.

thought that the increment in the doping concentration may carry the excitation energy to a luminescent killer centre [38]. However, in CL the quenching effect can be produced by several factors. One of them is by local heating that is caused by energetic electrons that impinge the luminescent material. Another factor is by saturation of luminescent centres, where the majority of them are in an excited state, leaving an insufficient number of them free in the ground state to accept energy from the excited carriers [39]. And the last factor might be due to the Auger effect; this produces the ejection of electrons leaving the luminescent centre de-excited [40]. Since both PL and CL quenching effects are similar, it is possible to say that these additional effects are not relevant in the present case.

The behaviour of the CL spectra for $HfO_2 : Sm^{3+}$ films, as a function of the wavelength, measured under steady-state excitation with accelerating beam voltages in the range from 4 to 14 kV is shown in figure 9. The shape observed in the emission spectra remains unaffected by the accelerating voltage, which consists of typical bands of the Sm^{3+} ions. However, the overall emission intensity is larger for higher electron accelerating voltages, showing no saturation effect in the voltage range studied. In principle, the incident electron beam reaches and penetrates the luminescent films to generate secondary electrons and electron–hole pairs which excite the activator ions in the host lattice to generate CL emissions. As the accelerating voltage increases, the penetrating electrons produce more electron–hole pairs due to their interaction with a larger volume of the luminescent material. In addition, there is a higher generation rate of every incident electron, resulting in a much more intense activator luminescence. Furthermore, it is possible that other emission mechanisms could be triggered since the e-beam energy is increased such as roentgenoluminescence generated x-rays produced by the de-acceleration of the incident electrons and the production of secondary electrons, which is important to the CL generation process, and they are generated along the entire zigzag path of energy dissipation, which may be many micrometres in length [41]. In these films the deposition temperature was 550 °C and the doping concentration was 3 a/o of $SmCl_3$.

The CL orange-reddish emissions could also be seen by the naked eye in normal room light, through the window of the CL chamber. Again, the above-mentioned is a rough indication of the strength of the CL emissions.

4. Conclusions

This paper reports on the structural and luminescent characteristics of $HfO_2 : Sm^{3+}$ films synthesized by the USP process. These films were rough but showed good adherence to the substrate and a high deposition rate of up to 2 μm per minute. The crystalline structure of the analysed coatings depended on the substrate temperature; at low temperatures (300–350 °C) they were in an amorphous state and when the deposition temperature was increased they were transformed, mainly, to a polycrystalline monoclinic phase of HfO_2. The PL and CL emission intensities increased as the deposition temperature was increased up to 550 °C. A concentration quenching, in both PL and CL, was observed if the activator concentration increased above the optimum doping concentration, 0.7 a/o, as measured by EDS. The CL emission intensity was found to increase as the electron accelerating voltage was raised. Also, the surface morphology of the coatings were dependent on T_s; SEM micrographs showed that these films were rough but continuous as the deposition temperature was increased. Finally, it was confirmed that hafnium oxide is an adequate host matrix to incorporate samarium ions as active centres and to originate strong orange-red PL and CL emissions. Therefore, this material could be a good candidate to be used in both applications involving photon or electron beam excitations.

Acknowledgments

The authors thank L Baños for XRD measurements. The technical support from M Guerrero and J García-Coronel is also appreciated. This work was partially supported by the CONACyT under project contract 48119. The financial support from SIP-IPN (grants 20060899 and 20071246) is also acknowledged.

References

[1] Capone S, Leo G, Rella R, Siciliano P, Vasanelli L, Alvisi M, Mirenghi L and Rizzo A 1998 *J. Vac. Sci. Technol.* A **16** 3564
[2] Waldorf A, Dobrowolski J A, Sullivan B T and Plante L M 1993 *Appl. Opt.* **32** 5583
[3] Ibégazéne H, Alpérine S and Diot C 1995 *J. Mater. Sci.* **30** 938
[4] Wang J, Li H P and Stevens R 1992 *J. Mater. Sci.* **27** 5397
[5] Wilk G D, Wallace R M and Anthony J M 2001 *J. Appl. Phys.* **89** 5243
[6] Niimistö L, Päiväsaari J, Niimistö J, Putkonen M and Nieminen M 2004 *Phys. Status Solidi* a **201** 1443
[7] Lehan J, Mao Y, Bovard B G and Macleod H A 1991 *Thin Solid Films* **203** 227
[8] Zukic M, Torr D G, Spann J F and Torr M R 1990 *Appl. Opt.* **29** 4284
[9] Edlou S M, Smajkiewicz A and Al-Jumaily G A 1993 *Appl. Opt.* **32** 5601
[10] Mignotte C 2001 *J. Non-Cryst. Solids* **291** 56
[11] Zhao X and Vanderbilt D 2002 *Phys. Rev.* B **65** 233106
[12] Lange S, Kiisk V, Reedo V, Kirm M, Aarik J and Sildos I 2006 *Opt. Mater.* **28** 1238
[13] Ito T, Maeda M, Nakamura K, Kato H and Ohki Y 2005 *J. Appl. Phys.* **97** 054104
[14] Kiisk V, Sildos I, Lange S, Reedo V, Tatte T, Kirm M and Aarik J 2005 *Appl. Surf. Sci.* **247** 412
[15] Villanueva-Ibañez M, Le luyer C, Dujardin C and Mugnier J 2003 *Mater. Sci. Eng.* B **105** 12
[16] Villanueva-Ibañez M, Le luyer C, Marty O and Mugnier J 2003 *Opt. Mater.* **24** 51
[17] García-Hipólito M, Alvarez-Fregoso O, Guzmán J, Martínez E and Falcony C 2004 *Phys. Status Solidi* a **201** R127
[18] Mikhail P, Hulliger J, Schnieper M and Bill H 2000 *J. Mater. Chem.* **10** 987
[19] Chukova O, Nedilco S, Moroz Z and Pashkovskyi M 2003 *J. Lumin.* **102–103** 498
[20] Lakshmanan A R 1999 *Prog. Mater. Science* **44** 1
[21] Lei B, Liu Y, Tang G, Ye Z and Shi C 2004 *Mater. Chem. Phys.* **87** 227
[22] Ritala M, Leskela M, Niinisto L, Prohaska T, Friedbacher G and Grasserbauer M 1994 *Thin Solid Films* **250** 72
[23] Balog M, Schieber M, Michman M and Patai S 1977 *Thin Solid Films* **41** 247
[24] Reicher D, Black P and Jungling K 2000 *Appl. Opt.* **39** 1589
[25] Cho Y J, Nguyen N V, Richter C A, Ehrstein J R, Lee B H and Lee J C 2002 *Appl. Phys. Lett.* **80** 1249
[26] García-Hipólito M, Caldiño U, Alvarez-Fragoso O, Alvarez-Pérez M A, Martínez-Martínez R and Falcony C 2007 *Phys. Status Solidi* a **204** 2355
[27] Perednis D and Gauckler L J 2005 *J. Electroceram.* **14** 103
[28] Esparza-García A E, García-Hipólito M, Aguilar-Frutis M A and Falcony C 2002 *Phys. Status Solidi* a **193** 117
[29] García-Hipólito M, Alvarez-Fregoso O, Martínez E, Falcony C and Aguilar-Frutis M A 2002 *Opt. Mater.* **20** 113
[30] García-Hipólito M, Hernández-Pérez C D, Alvarez-Fregoso O, Martínez E, Guzmán-Mendoza J and Falcony C 2003 *Opt. Mater.* **22** 345
[31] Langlet M and Joubert J C 1993 *Chemistry of Advanced Materials* ed C N R Rao (Oxford: Blackwell Science) p 55
[32] Messing G L, Zhang S and Jayanthi G V 1993 *J. Am. Ceram. Soc.* **76** 2707
[33] Newport A, Silver J and Vecht A 2002 *J. Electrochem. Soc.* **147** 3944
[34] Annapurna K, Dwivedi R N, Kundu P and Buddhudu S 2003 *Mater. Res. Bull.* **38** 429
[35] May P S, Matcalf D H, Richardson F S, Carter R C, Miller C E and Palmer R A 1992 *J. Lumin.* **51** 249
[36] Devline K, O'Kelly B, Tang Z R, McDonagh C and McGlip J F 1991 *J. Non-Cryst. Solids* **135** 8
[37] Dexter D L and Schulman J H 1954 *J. Chem. Phys.* **22** 1063
[38] Hase T, Kano T, Nakasawa E and Yamamoto H 1990 *Phosphors Materials for Cathode-Ray Tubes (Advances in Electronics and Electron Physics* vol 79) (New York: Academic) p 271
[39] de Leeuw D M and Thoof G W 1983 *J. Lumin.* **28** 275
[40] Imanaga S, Yocono S and Hosima T 1980 *Japan. J. Appl. Phys.* **19** 41
[41] Myhajlenco S 1998 *Luminescence of Solids* ed D R Vij (New York: Plenum) chapter 4